RESEARCH PAPER

Reusable (MWCNTs)-COOH/Fe$_3$O$_4$-CaO Magnetic Nanostructure Promoted Three-Component Synthesis of Hexahydroacridine Derivatives

Omekolsoom Shabani, Navabeh Nami *, Rahimeh Hajinasiri, Masoumeh Hosseinzadeh

Department of Chemistry, Qaemshahr Branch, Islamic Azad University, Qaemshahr, Iran

ABSTRACT

(MWCNTs)-COOH/Fe$_3$O$_4$-CaO magnetic nanostructure was employed for the high-yield synthesis of hexahydroacridine-1,8-dione derivatives via three-component reaction of dimedone, unprotected sugars, and aniline or 4-bromoaniline in ethanol under reflux conditions. (MWCNTs)-COOH/Fe$_3$O$_4$-CaO was prepared by COOH functionalized multi-walled carbon nanotubes (MWCNTs)-COOH with Fe$_3$O$_4$-CaO nanoparticles in the presence of FeSO$_4$ and eggshell. This heterogeneous hybrid nanostructure, (MWCNTs)-COOH/Fe$_3$O$_4$-CaO, was determined by SEM, TEM, XRD, EDX, FT-IR, and TGA. The potential application of this covalently linked basic catalyst was also investigated as an efficient, recyclable, and heterogeneous catalyst for the synthesis of hexahydroacridine-1,8-dione. The condensation of dimedone with unprotected sugars and aniline or 4-bromoaniline in the presence of a catalytic amount of (MWCNTs)-COOH/Fe$_3$O$_4$-CaO magnetic nanostructure gave hexahydroacridine-1,8-dione derivatives in good yields. The products were identified by FT-IR, NMR spectra, and elemental analysis. The catalyst was separated by an external magnet from the reaction mixture, washed, and dried at 100 °C for 2 h. The recovered catalyst was then re-entered into a fresh reaction mixture and recycled 5 times without considerable loss of activity.

INTRODUCTION

In recent years, the combination of carbon nanotubes (CNTs) and inorganic nanoparticles have formed nanostructures that have superior properties [1]. Multi-walled carbon nanotubes have gained more interest than others, based on their great potentialities in various technological fields such as controlled drug release, wide surface area, chemical, electrical, thermal performance, and heterogeneous catalysis [2–6]. The greatest advantages of heterogeneous catalysts are the ease of separation from the reaction mixture and reuse [7,9]. However, the most important problem concerning MWCNTs lies within their separation from aqueous solution [10]. To overcome the poor processability and dispersibility, the functionalization and solubilization of CNTs have received much attention. The decoration of CNTs with inorganic compounds through covalent and non-covalent bonds can give them new properties and potential for various new applications [11]. The reaction of bimetal oxides like Fe$_3$O$_4$-CaO

* *Corresponding Author Email: navabehnami@yahoo.com*

nanoparticles and multi-walled carbon nanotubes to form new type of hybrid nanostructure materials will exploit even more diverse applications [12].

Fe$_3$O$_4$ magnetic nanoparticles were used in most studies due to high saturation magnetization, high magnetic susceptibility, chemical stability, and biocompatibility. Fe$_3$O$_4$ MNPs have been used in gene delivery, cell therapy, drug delivery, recording material, sensor, and catalyst [13-18]. These magnetic nanoparticles have been used as an efficient catalyst in many organic reactions [19]. Fe$_3$O$_4$ MNPs tend to aggregate to form the bulk metal oxide, giving rise to a dramatic decrease in surface area. To prevent this undesirable metal oxide aggregation, magnetic cores have been surrounded by functional ligands such as ligands that contain terminal amine, phosphoric acid, thiol, or carboxylic acid groups [20,21]. They can bind with the surface of magnetic nanoparticles. Magnetic metal oxide NPs immobilized acid functionalized multi-walled carbon nanotubes (MWCNTs)-COOH have shown superior catalytic activities for the synthesis of organic reactions, due to the presence of a very active site on the large surface of (MWCNTs–NPs) hybrid structures [22,23]. On the other hand, CaO was often used as a heterogeneous catalyst because of its low toxicity, regeneration, high basicity, and high catalytic activity [24]. However, the shortcomings possessed by CaO are low thermal stability and low mechanical strength, so it needs to be impregnated with other oxides [25]. CaO can be easily derived from the environment, waste sources such as ashes, crab shells, sand, oyster shells, animal bones, snail shells, and also eggshells [26-30]. The most chemical component of the calcined waste eggshell is CaO (about 97%), which can be obtained from calcium carbonate in the eggshell under high temperatures (in the range of 700–1000 °C) [31]. Because of the above reasons and due to the presence of the high surface area of MWCNT–COOH/Fe$_3$O$_4$-CaO hybrid, it can be employed as alternative catalyst support, because of their high surface area resulting in high catalyst loading capacity, high dispersion, outstanding stability, and convenient catalyst recycling. We proposed that the MWCNT–COOH/Fe$_3$O$_4$-CaO hybrid can increase the catalytic properties for the synthesis of hexahydroacridine-1,8-dione derivatives. hexahydroacridine-1,8-dione derivatives have been extensively studied due to their wide range of biological activities and pharmaceutical properties,

such as anticancer, antimicrobial, anti-Alzheimer, antibiotic, antileishmanial, and antimalarials agents [32,33]. There are various reports in the literature on the three-component Hantzsch-type synthesis of acridines involving condensation of aromatic aldehydes, anilines, and dimedone via conventional methods [34]. However, many of these methods suffered some limitations. So in this article, we present a simple, cheap, and eco-friendly synthesis of hexahydroacridine-1,8-dione derivatives using (MWCNTs)-COOH/Fe$_3$O$_4$-CaO hybrid as an effective catalyst under mild reaction conditions and good yields.

MATERIALS AND METHODS
Chemicals and Instrumentation

Solvents and chemicals were purchased from Aldrich and Merck. (MWCNTs)-COOH (OD: 20-30 nm) was purchased from US Research Nanomaterials, Inc. (MWCNTs)-COOH/Fe$_3$O$_4$-CaO was distinguished by powder X-ray diffraction (XRD) PW 3040/60 X'Pert PRO diffractometer system, using Cu Ka radiation with (λ = 1.5418 Å) in the range of 2θ = 20–80° at room temperature. The morphology and sizes of NPs were measured using a transmission electron microscope (TEM, 150 kV, and Philips-CM 10) and a scanning electron microscope (SEM) by Daypetronic Company-Iran. FT-IR measurements were recorded on a Shimadzu 8400s spectrometer with KBr plates. The NMR spectra were determined on Bruker XL 400 (400 MHz) instruments; Mass-spectrometric measurements were made on an Agilent 6890 N Network GC system. The elemental analysis was performed by the microanalytical service of the Daypetronic Company. Melting points were obtained on an Electrothermal 9100 without further corrections.

Preparation of (MWCNTs)-COOH/Fe$_3$O$_4$-CaO hybrid

Waste quail eggshells were thoroughly cleaned and air-dried after the removal of the inner membrane layer. Cleaned eggshells were crushed into small pieces and dried at 80°C for 24 h in the oven. The functionalize (MWCNTs)-COOH (0.3 g), the dried eggshells (0.1 g), and FeSO$_4$ (0.1 g) were added to 50 ml of acetic acid in a flask. The mixture was kept in an ultrasonic bath for 30 min and then slowly stirred outside the ultrasonic device for another 2 hours, under reflux conditions. The solvent was evaporated and The resulting precipitate was calcined at 250°C for 3 hours to
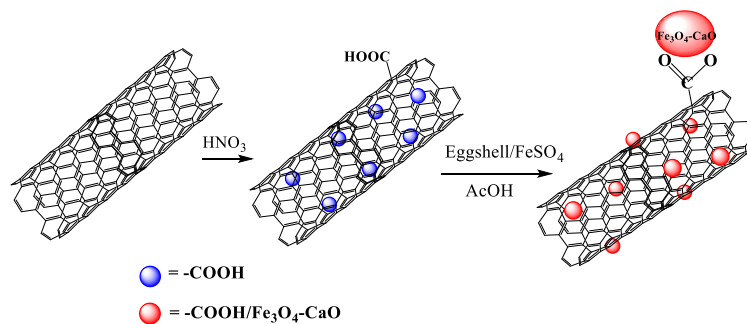
Fig. 1. Preparation of (MWCNTs)-COOH/Fe₃O₄-CaO nanomaterial.

obtain magnetically (MWCNTs)-COOH/Fe$_3$O$_4$-CaO (Fig. 1).

General procedure for the synthesis of compounds 1-5 in the presents of (MWCNTs)-COOH/Fe$_3$O$_4$-CaO

Raw materials and (MWCNTs)-COOH/Fe$_3$O$_4$-CaO (7 mol%) were mixed and reacted in ethanol (10 ml) under reflux conditions. The completion of the reaction was determined by TLC using *n*-hexane: ethyl acetate (2:1) and appeared by a UV lamp (254 & 366 nm). In the end, the catalyst was separated by an external magnet, filtered, washed with ethanol and water, dried at 80 °C for 1h, and reused for the same reaction. The residue of the reaction mixture was evaporated, and the crude product was purified by short-column chromatography on silica gel (CHCl$_3$: MeOH / 10:1). This column chromatography operation was repeated to give pure compounds (1-5) as colorless, viscous oils. The products were determined by CHN analyses, NMR, and FT-IR spectra.

10-(4-bromophenyl)-9-((R)-((2S,3S,4R)-3,4-dihydroxytetrahydrofuran-2-yl)(hydroxy)methyl)-3,3,6,6-tetramethyl-3,4,6,7,9,10-hexahydroacridine-1,8(2H,5H)-dione 1

Reaction of d-mannose (1 mmol), dimedone (2 mmol), and 4-bromoaniline (1 mmol), yellow powder. FT-IR spectrum, v, cm^{-1}: 3420.8 (OH), 3061.7 (CH$_{aro}$), 2955.4 (CH$_{aliph}$), 2869.2 (CH$_{aliph}$), 1740.1 (C=O), 1622.0 (C=C), 1489.5 (C=C), 1398.8 (C=C), 1262.6 (C-O), 1223.1 (C-O), 1771.5 (C-O), 1146.5 (C-O), 1070.4 (C-O), 1036.1 (C-O). ^{1}H NMR spectrum (400 MHz, DMSO-*d*6), δ ppm (*J*, Hz): 7.11 (2H, d, *J* = 8.8 Hz, CH$_{aro}$), 6.50 (2H, d, *J* = 8.4 Hz, CH$_{Aro}$), 5.25 (2H, br, OH), 4.28 (1H, t, *J* = 7.6 Hz, CH), 4.15 (1H, d, *J* = 6.4 Hz, CH), 3.65 (1H, d, *J* = 8.4 Hz, CH), 3.57 (1H, d, *J* = 8.4 Hz, CH$_2$), 3.34 (2H,

t, *J* = 9.2 Hz, CH), 2.23 (1H, d, *J* = 16.0 Hz, CH$_2$), 2.16 (1H, d, *J* = 16.0 Hz, CH$_2$), 2.09 (1H, d, *J* = 14.4 Hz, CH$_2$), 2.02 (1H, d, *J* = 14.4 Hz, CH$_2$), 1.94 (3H, t, *J* = 16.2 Hz, CH$_2$), 1.09 (3H, s, CH$_3$), 1.00 (3H, s, CH$_3$), 0.94 (6H, s, 2CH$_3$). ^{13}C NMR spectrum (100 MHz, DMSO-*d*6), δ, ppm: 193.01, 184.97, 171.56, 145.09, 138.05, 132.02, 124.98, 116.18, 113.59, 110.91, 93.49, 81.09, 70.03, 64.21, 51.60, 49.25, 34.51, 28.81. Found, %: C, 60.47; H, 6.21; N, 2.53. C$_{28}$H$_{34}$BrNO$_6$ (559.16). Calculated, %: C, 60.00; H, 6.11; N, 2.50.

10-(4-bromophenyl)-9-((S)-((2S,3S,4R)-3,4-dihydroxytetrahydrofuran-2-yl) (hydroxy) methyl)-3,3,6,6-tetramethyl-3,4,6,7,9,10-hexahydroacridine-1,8(2H,5H)-dione 2

Reaction of d-galactose (1 mmol), dimedone (2 mmol), and 4-bromoaniline (1 mmol), yellow powder. FT-IR spectrum, v, cm^{-1}: 3404.1 (OH), 3369.8 (OH), 3012.4 (CH$_{aro}$), 2953.9 (CH$_{aliph}$), 2874.8 (CH$_{aliph}$), 1699.7 (C=O), 1619.9 (C=C), 1489.2 (C=C), 1402.0 (C=C),1260.6 (C-O), 1223.7 (C-O), 1172.4 (C-O), 1069.6 (C-O), 1031.7 (C-O). ^{1}H NMR spectrum (400 MHz, DMSO-*d*6), δ ppm (*J*, Hz): 7.12 (2H, d, *J* = 8.8 Hz, CH$_{aro}$), 6.50 (2H, d, *J* = 8.4 Hz, CH$_{Aro}$), 5.25 (2H, br, OH), 4.66 (1H, d, *J* = 8.0 Hz, CH), 4.37 (1H, d, *J* = 7.2 Hz, CH), 3.72 (1H, t, *J* = 5.2 Hz, CH), 3.45 (1H, t, *J* = 9.6 Hz, CH$_2$), 3.40 (1H, br, CH), 2.24 (1H, d, *J* = 16 Hz, CH$_2$), 2.13 (1H, d, *J* = 16 Hz, CH$_2$), 1.98 (3H, br, CH$_2$), 1.93 (1H, d, *J* = 8.8 Hz, CH$_2$), 1.86 (1H, d, *J* = 10.0 Hz, CH$_2$), 1.06 (3H, s, CH$_3$), 1.00 (3H, s, CH$_3$), 0.93 (6H, s, 2CH$_3$). ^{13}C NMR spectrum (100 MHz, DMSO-*d*6), δ, ppm: 192.45, 186.64, 175.25, 149.11, 146.77, 131.69, 121.97, 116.19, 115.62, 111.86, 110.72, 101.69, 90.53, 70.86, 69.99, 63.52, 51.60, 34.20, 31.88, 28.36. Found, %: C, 60.36; H, 6.15; N, 2.47. C$_{28}$H$_{34}$BrNO$_6$ (559.16). Calculated, %: C, 60.00; H, 6.11; N, 2.50.

10-(4-bromophenyl)-9-((2S,3S,4R)-3,4-dihydroxytetrahydrofuran-2-yl)-3,3,6,6-tetramethyl-3,4,6,7,9,10-hexahydroacridine-1,8(2H,5H)-dione 3

Reaction of d-arabinose (1 mmol), dimedone (2 mmol), and 4-bromoaniline (1 mmol), yellow powder. FT-IR spectrum, ν, cm⁻¹: 3417.8 (OH), 3015.9 (CH$_{aro}$), 2955.4 (CH$_{aliph}$), 2873.3 (CH$_{aliph}$), 1705.2 (C=O), 1616.9 (C=C), 1485.0 (C=C), 1402.6 (C=C),1262.4 (C-O), 1224.4 (C-O), 1171.9 (C-O),1147.3 (C-O), 1078.1 (C-O), 1035.3 (C-O). ¹H NMR spectrum (400 MHz, DMSO-*d*6), δ ppm (*J*, Hz): 7.11 (2H, d, *J* = 8.8 Hz, CH$_{aro}$), 6.50 (2H, d, *J* = 8.8 Hz, CH$_{Aro}$), 5.25 (2H, br, OH), 4.62 (1H, t, *J* = 5.6 Hz, CH), 4.38 (1H, d, *J* = 8.0 Hz, CH), 3.57 (1H, d, *J* = 8.4 Hz, CH), 3.38 (2H, m, CH$_2$), 3.21 (1H, d, *J* = 8.4 Hz, CH), 2.19 (2H, d, *J* = 11.6 Hz, CH$_2$), 1.94 (3H, t, *J* = 5.6, CH$_2$), 1.89 (2H, s, CH$_2$), 1.06 (3H, s, CH$_3$), 1.00 (3H, s, CH$_3$), 0.92 (6H, s, 2CH$_3$). ¹³C NMR spectrum (100 MHz, DMSO-*d*6), δ, ppm: 192.60, 186.96, 176.41, 148.53, 131.77, 116.20, 116.05, 109.87, 106.42, 90.51, 72.68, 71.54, 64.33, 51.61, 49.47, 37.97, 35.29, 34.19, 31.83, 29.40, 28.98, 28.51. Found, %: C, 61.28; H, 6.17; N, 2.69. C$_{27}$H$_{32}$BrNO$_5$ (530.46). Calculated, %: C, 61.14; H, 6.08; N, 2.64.

10-(4-bromophenyl)-9-((2S,3S,4R)-3,4-dihydroxytetrahydrofuran-2-yl)-3,3,6,6-tetramethyl-3,4,6,7,9,10-hexahydroacridine-1,8(2H,5H)-dione 4

Reaction of d-ribose (1 mmol), dimedone (2 mmol), and 4-bromoaniline (1 mmol), yellow

powder. FT-IR spectrum, ν, cm⁻¹: 3393.5 (OH), 3019.0 (CH$_{aro}$), 2954.6 (CH$_{aliph}$), 2876.3 (CH$_{aliph}$), 1710.7 (C=O), 1600.8 (C=C), 1474.3 (C=C), 1395.9 (C=C), 1220.5 (C-O), 1171.6 (C-O), 1147.9 (C-O), 1082.1 (C-O), 1035.5 (C-O). ¹H NMR spectrum (400 MHz, DMSO-*d*6), δ ppm (*J*, Hz): 7.11 (2H, d, *J* = 8.8 Hz, CH$_{aro}$), 6.50 (2H, d, *J* = 8.8 Hz, CH$_{Aro}$), 5.26 (2H, br, OH), 4.60 (1H, dd, *J* = 4.4, 7.2 Hz, CH), 4.31 (1H, d, *J* = 7.2 Hz, CH), 3.57 (1H, dd, *J* = 4.4, 6.4 Hz, CH), 3.42-3.35 (2H, m, CH), 2.25 (1H, d, *J* = 16.8 Hz, CH$_2$), 2.01 (4H, s, CH$_2$), 1.94 (2H, d, *J* = 18.2, CH$_2$), 1.85 (1H, d, *J* = 14.8 Hz, CH$_2$), 1.05 (3H, s, CH$_3$), 1.00 (3H, s, CH$_3$), 0.93 (6H, s, 2CH$_3$). ¹³C NMR spectrum (100 MHz, DMSO-*d*6), δ, ppm: 192.54, 174.95, 131.76, 116.20, 115.42, 111.50, 91.59, 73.17, 71.82, 63.64, 51.50, 48.73, 37.80, 34.67, 34.18, 31.89, 29.49, 28.79, 28.26. Found, %: C, 61.33; H, 6.02; N, 2.68. C$_{27}$H$_{32}$BrNO$_5$ (530.46). Calculated, %: C, 61.14; H, 6.08; N, 2.64.

9-((S)-hydroxy((2S,3S,4R)-4-hydroxy-3-(((2R,3R,4S,5S,6R)-3,4,5-trihydroxy-6-(hydroxyl methyl)tetrahydro-2H-pyran-2-yl)oxy) tetrahydrofuran-2-yl)methyl)-3,3,6,6-tetramethyl-10-phenyl-3,4,6,7,9,10-hexahydroacridine-1,8(2H,5H)-dione 5

Reaction of maltose (1 mmol), dimedone (2 mmol), and aniline (1 mmol), yellow powder. FT-IR spectrum, ν, cm⁻¹: 3415.6 (OH), 3017.4 (CH$_{aro}$), 2955.5 (CH$_{aliph}$), 2928.8 (CH$_{aliph}$), 1728.8 (C=O), 1603.2 (C=C), 1473.1 (C=C), 1404.2 (C=C), 1268.5 (C-N), 1145.8 (C-O), 1120.7 (C-O), 1071.7
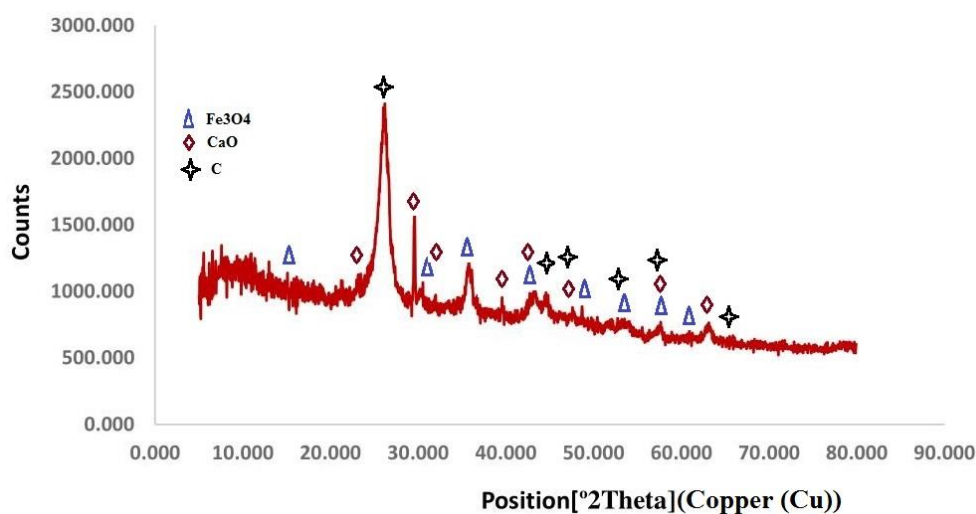

Fig. 2. XRD of (MWCNTs)-COOH/Fe₃O₄-CaO.

(C-O), 1033.0 (C-O). ^{1}H NMR spectrum (400 MHz, DMSO-*d*6), δ ppm (*J*, Hz): 7.35 (2H, t, *J* = 7.6 Hz, CH$_{aro}$), 7.17 (2H, d, *J* = 7.6 Hz, CH$_{aro}$), 7.13 (1H, t, *J* = 8.0 Hz, CH$_{Aro}$), 4.90 (4H, br, OH), 4.19 (1H, d, *J* = 8.0 Hz, CH), 4.13 (1H, br, OH), 3.70 (2H, d, *J* = 4.8 Hz, CH), 3.57 (2H, d, *J* = 18.8 Hz, CH), 3.42-3.49 (6H, br, CH), 3.13 (1H, t, *J* = 6.0 Hz, CH), 3.04 (1H, t, *J* = 9.2 Hz, CH), 2.20 (2H, q, *J* = 12.4 Hz, CH$_2$), 2.05 (2H, s, CH$_2$), 1.95 (2H, d, *J* = 12.4 Hz, CH$_2$), 1.90 (4H, br, CH$_2$), 1.35 (1H, m, CH$_2$), 1.28 (2H, br, CH$_2$), 1.05 (3H, s, CH$_3$), 0.99 (3H, s, CH$_3$), 0.90 (6H, s, 2CH$_3$). ^{13}C NMR spectrum (100 MHz, DMSO-*d*6), δ, ppm: 192.45, 179.16, 167.45, 132.16, 129.65, 129.12, 116.20, 100.46, 91.86, 79.62, 73.87, 73.64, 72.94, 70.39, 63.42, 51.72, 38.52, 34.16, 31.64, 30.24, 29.27, 28.81, 28.57, 23.69, 22.86. Found, %: C, 63.39; H, 7.15; N, 2.29. C$_{34}$H$_{45}$NO$_{11}$ (503.22). Calculated, %: C, 63.44; H, 7.05; N, 2.18.

RESULTS AND DISCUSSION

The present paper reports the results of research aimed to verify the activity of the (MWCNT)-COOH/Fe$_3$O$_4$-CaO hybrid as an effective catalyst in the synthesis of hexahydroacridine-1,8-dione derivatives. The possible interaction between eggshells, FeSO$_4$, and (MWCNTs)-COOH was investigated using TGA/DTA, XRD, TEM, SEM, EDX, and FT-IR spectroscopy.
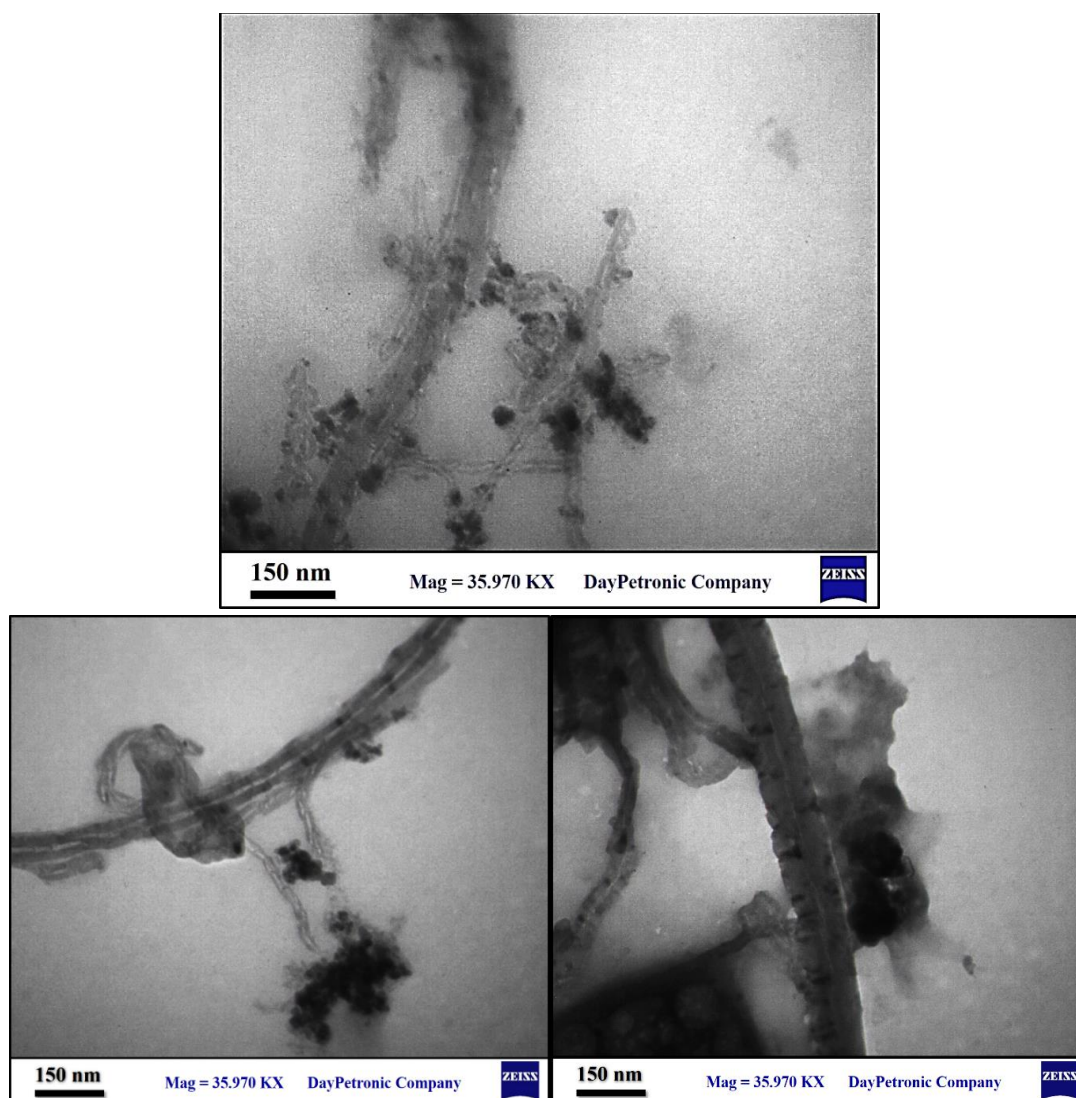

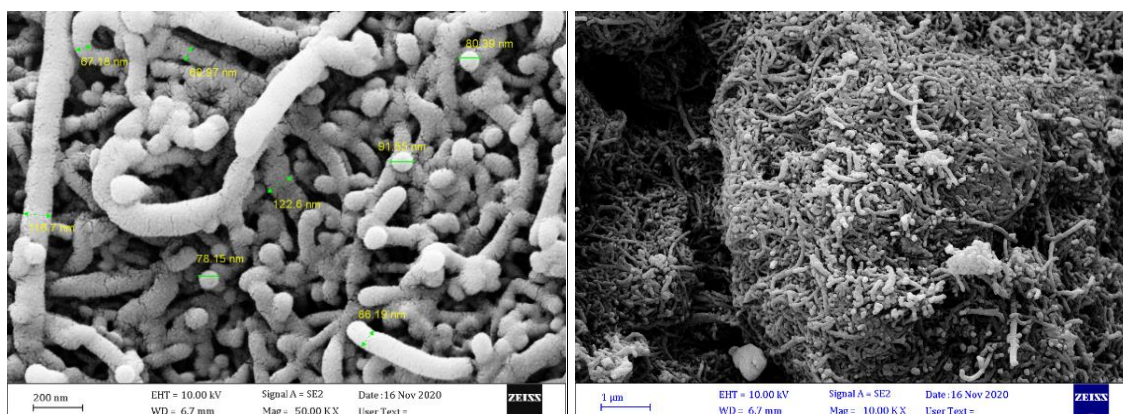Fig. 3. TEM image of (MWCNTs)-COOH/Fe$_3$O$_4$-CaO nanomaterial.

Fig. 4. FESEM micrograph of (MWCNTs)-COOH/Fe$_3$O$_4$-CaO nanomaterial

(MWCNTs)-COOH/Fe$_3$O$_4$-CaO characterization

The typical FT-IR spectra of (MWCNTs)-COOH/Fe$_3$O$_4$-CaO can be clarified briefly.

the vibration of the carbon skeleton of the carbon nanotubes was shown at around 1300-1550 cm^{-1}. The bands at about 1630-1750 and 1000-1300 cm^{-1} indicate the existence of C=O groups of (MWCNTs)–COOH [35]. The bands at about 2000-2450 cm^{-1} are belonged to the C=C double bonds stretch vibration from the surface of the MWCNTs [36]. The weak peaks around 3500-3900 cm^{-1} can be assigned to the stretching vibrations of OH groups [37]. The absorption band at 400–700 cm^{-1} is related to the Fe-O and Ca-O, which confirms the formation of the Fe$_3$O$_4$-CaO MNPs.

X-ray diffraction (XRD) is normally used to study and characterize the crystallization and average size of (MWCNTs)-COOH/Fe$_3$O$_4$-CaO. In Fig. 2, the XRD pattern of (MWCNTs)-COOH/Fe$_3$O$_4$-CaO demonstrates seven intense peaks in the whole spectrum of 2θ values ranging from 5˚ to 80˚. The presence of eight distinct high diffraction peaks at 2θ values of 23.08˚, 43.15˚, 47.84˚, and 57.37˚ for carbon, 29.52˚, 35.94˚, 39.44˚, 48.67˚ for CaO, and 30.36˚, 35.76˚, 43.47˚, 57.51˚, and 63.16˚ for Fe$_3$O$_4$ respectively, (JCPDS Number. C: 00-026-1080, Fe$_3$O$_4$: 01-075-0449, and JCPDS Number. CaO: 98-000-5337) [38,39] confirmed that the (MWCNTs)-COOH/Fe$_3$O$_4$-CaO had been formed. The other diffraction peaks could be due to some chemical compounds and crystals on the surface of the nanoparticle. The wide X-ray

diffraction peaks around their bases show that the (MWCNTs)-COOH/Fe$_3$O$_4$-CaO is in nano sizes. With the XRD pattern, the average diameter which can be calculated from the Scherrer equation [40] (D=Kλ/βcosθ, where β is the peak width at half maximum, λ is X-ray wavelength, and K is constant) is obtained at about 13.7 nm for Fe$_3$O$_4$-CaO NPs. The crystallite size was calculated based on the diffraction peak at a 2θ value of 35.75 These nanoparticles have been fixed on the different layers of carbon nanotubes and increased the outer diameter of the nanotubes (about 70-100 nm, Fig. 2).

The morphology and size of (MWCNTs)-COOH/Fe$_3$O$_4$-CaO were studied using transmission electron microscopy (TEM) in Fig. 3. The TEM image indicates that the Fe$_3$O$_4$-CaO nanoparticles are well bonded to the surface of multi-wall carbon nanotubes. On the other hand, TEM values are in good agreement with XRD.

Fig. 4 shows the SEM images of (MWCNTs)-COOH/Fe$_3$O$_4$-CaO. The outside diameter (OD) of (MWCNTs)-COOH was 20-30 nm but after modification, it was changed to 70-100 nm. It is shown that Fe$_3$O$_4$-CaO nanoparticles have grown as nanoparticles on the surface and inside of the (MWCNTs)-COOH.

In Fig. 5, EDX analysis was performed to confirm the elements present in the resulting (MWCNTs)-COOH/Fe$_3$O$_4$-CaO. For using SEM/EDS to analyse the composition of a sample, usually a heavy metal such as Au (Au-Pd) was coated the sample to make it conductive before insert it into FE-SEM. Therefore, there is a signal of coating metal
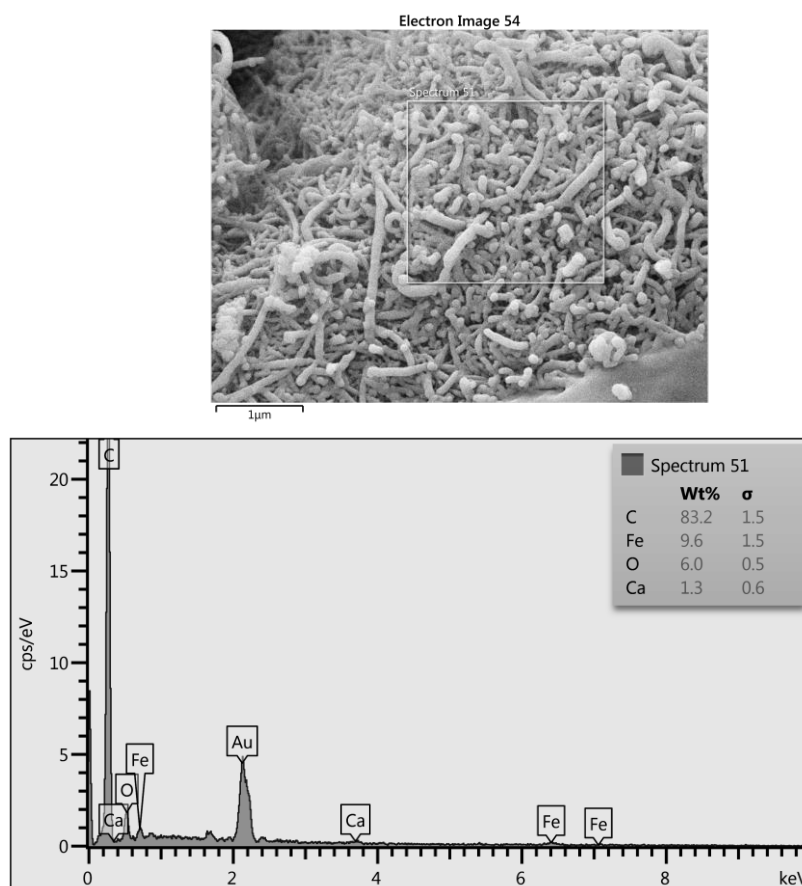
Fig. 5. EDX of (MWCNTs)-COOH/Fe$_3$O$_4$-CaO nanomaterial.

(Au) in EDX. In addition, the analysis reveals the presence of Fe, Ca, O, and C which emphasizes the success of the decoration process with Fe$_3$O$_4$-CaO nanoparticles.

Fig. 6 shows the saturation magnetization (Ms) values of the magnetic (MWCNTs)-COOH/Fe$_3$O$_4$-CaO and pure Fe$_3$O$_4$ NPs measured. All of the samples exhibited typically superparamagnetic features with negligible of coercivity and remanence. As shown in Fig. 6, the Ms of the (MWCNTs)-COOH/Fe$_3$O$_4$-CaO was weakened to a large extent when compared with that of pure Fe$_3$O$_4$ NPs. (MWCNTs)-COOH, the magnetic Fe$_3$O$_4$ NPs, and CaO NPs can cause the coating effect, which leads to the reduction of the magnetic responsiveness. However, this value is high enough for the nanostructure to be separated from the reaction mixture by an external magnet.

The catalytic activity of (MWCNTs)-COOH/Fe$_3$O$_4$-CaO and heterocyclic compounds characterization

(MWCNTs)-COOH/Fe$_3$O$_4$-CaO (7 mol%) was used as an efficient catalyst for the synthesis of hexahydroacridine-1,8-dione derivatives. Because of its excellent capacity, the exceedingly simple workup and good yields (MWCNTs)-COOH/Fe$_3$O$_4$-CaO was proved to be a good catalyst for these reactions.

In the preliminary stage of the investigation, the model reaction of 4-bromoaniline, arabinose, and dimedone (Fig. 7) was carried out by using various amounts of (MWCNTs)-COOH/Fe$_3$O$_4$-CaO in various solvents and solvent-free conditions. As shown in Table 1, the optimum amount of catalyst was 7 mol%. Decreasing the amount of catalyst leads to a decrease in the yield of the reaction while increasing the amount of catalysts, the optimum amount of (MWCNTs)-COOH/Fe$_3$O$_4$-CaO was 7 mol% as shown in Table 2. Increasing the amount of the catalyst to more than 7 mol% does not improve the yield of the product any further.
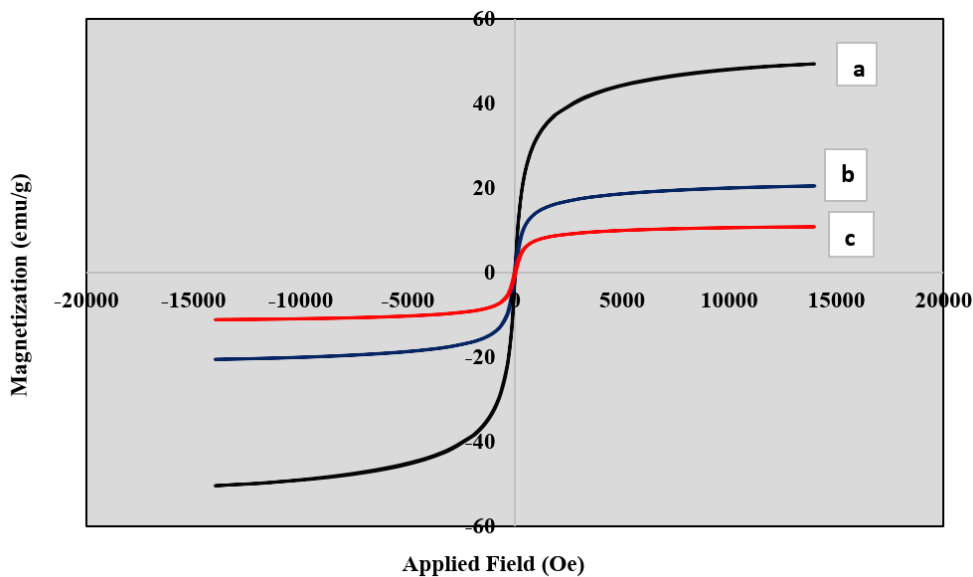
Fig. 6. VSM results of (a) Fe$_3$O$_4$ MNPs, (b) Fe$_3$O$_4$-CaO MNPs, (c) (MWCNTs)-COOH/Fe$_3$O$_4$-CaO Magnetic hybrid nanomaterial.

In the absence of (MWCNTs)-COOH/Fe$_3$O$_4$-CaO, the result of the reaction on the TLC plate even after 4h of the reaction wasn't good. The best yield of the product was acquired with 7 mol% of (MWCNTs)-COOH/Fe$_3$O$_4$-CaO in EtOH under mild reaction conditions (Table 1, Entry 9). It is important to note that, under the same conditions, (MWCNTs)-COOH or Fe$_3$O$_4$-CaO NPs displayed almost no activity. D-arabinose did not react with dimedone and the yield of the reaction did not exceed more than 10% even after 6 h. It is clear that modification of (MWCNTs)-COOH with Fe$_3$O$_4$-CaO remarkably increased its catalytic activity.

The inductively coupled plasma–atomic emission spectroscopy (ICP-AES) analysis was performed to determine the amount of Fe and Fe$_3$O$_4$-CaO loading in (MWCNTs)-COOH/Fe$_3$O$_4$-CaO before (6.74 mg/g) and after (6.62 mg/g) the reaction.

The leaching of the catalyst has been measured by using a hot filtration method. The reaction mixture has been filtered out the catalyst ((MWCNTs)-COOH/Fe$_3$O$_4$-CaO) from the reaction mixture at the stage of 50% conversion. We did not observe further progress of the reaction after filtration which indicates there was no leaching
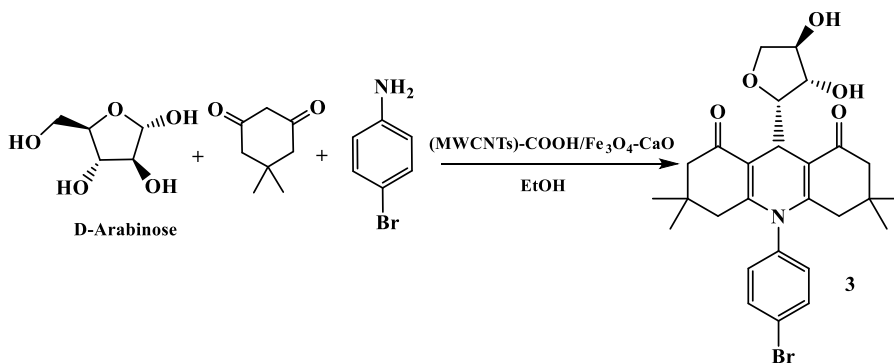

Fig. 7. Synthesis of 10-(4-bromophenyl)-9-((2S,3S,4R)-3,4-dihydroxytetrahydrofuran-2-yl)-3,3,6,6-tetramethyl-3,4,6,7,9,10-hexahydroacridine-1,8(2H,5H)-dione 3.

Table 1. The reaction of 4-bromoaniline, d-arabinose (1 mmol), and dimedone (1 mmol) under different conditions.

Entry	Solvent	MWCNTs)-COOH/ Fe₃O₄-CaO (mol%)	Time (hour)	Yield^a (%)
1	THF$_{dry}$	-	4	trace
2	THF$_{dry}$	3	3	32
3	THF$_{dry}$	5	3	56
4	THF$_{dry}$	7	3	83
5	THF$_{dry}$	10	3	83
6	EtOH	-	4	trace
7	EtOH	3	3	52
8	EtOH	5	3	72
9	EtOH	7	2	95
10	EtOH	10	2	96
11	H₂O	-	4	trace
12	H₂O	3	3	38
13	H₂O	5	3	41
14	H₂O	7	3	57
15	H₂O	10	3	57
16	CH₂Cl₂ dry	-	4	trace
17	CH₂Cl₂ dry	3	3	33
18	CH₂Cl₂ dry	5	3	45
19	CH₂Cl₂ dry	7	3	52
20	CH₂Cl₂ dry	10	3	53
21	CH₃CN	-	4	trace
22	CH₃CN	3	3	42
23	CH₃CN	5	3	57
24	CH₃CN	7	3	61
25	CH₃CN	10	3	61
26	DMF	-	3	trace
27	DMF	3	4	46
28	DMF	5	3	53
29	DMF	7	3	71
30	DMF	10	3	70
31	Solvent-free	-	3	47
32	Solvent-free	3	3	52
33	Solvent-free	5	3	64
34	Solvent-free	7	3	77
35	Solvent-free	10	3	78

^{a} Isolated yield
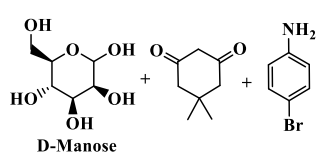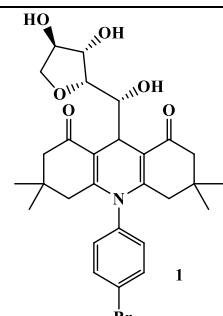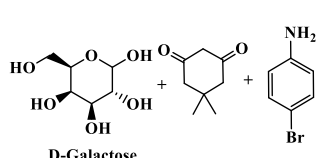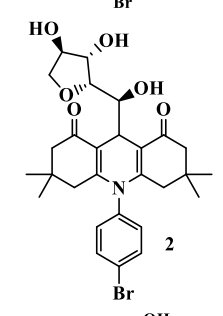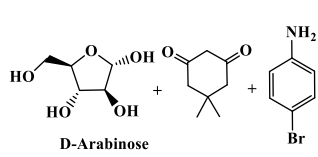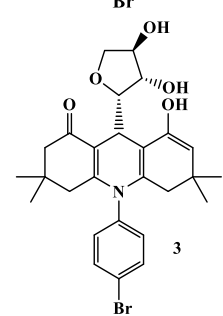
to confirm the absence of Fe₃O₄-CaO NPs and stability of the catalyst.

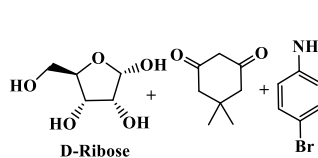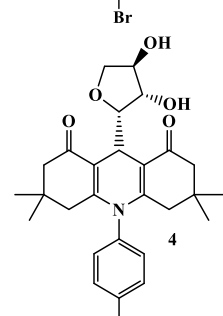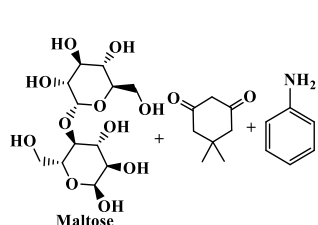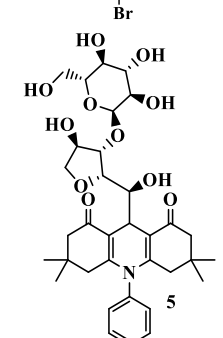We extended our study to different organic reactions to evaluate the scope and potential limitations of this methodology (Table 2, entries 1–5). In almost all cases, the reactions proceeded smoothly within 2-3 hours, providing the corresponding products in good isolated yields. The products were isolated, purified, and analysed by NMR and IR. For example, the ¹H NMR spectrum of 10-(4-bromophenyl)-9-((2S,3S,4R)-3,4-dihydroxytetrahydrofuran-2-yl)-3,3,6,6-tetramethyl-3,4,6,7,9,10-hexahydroacridine-1,8(2H,5H)-dione 3 (Fig. 8) shows singlets at 5.25 and 4.62 ppm for OH protons, 3.57, 3.38, and 3.21 ppm for CH protons. Three singlet signals attributed to Me protons have appeared at 1.06, 1.00, and 0.92 ppm, respectively.

In the ¹³C NMR spectrum (Fig. 9), the resonances related to CH₃ and CH₂ carbon groups of 3 were appeared at 37.97, 35.29, 34.19, 31.83, 29.40, 28.98, and 28.51 ppm, respectively. The signals

Table 2. Synthesis of hexahydroacridine-1,8-dione derivatives using (MWCNTs)-COOH/Fe₃O₄-CaO.

Entry	Raw Materials	Product	Time (h)/	Yield%
1	D-Manose	**1**	2	91
2	D-Galactose	**2**	2	96
3	D-Arabinose	**3**	2	95
4	D-Ribose	**4**	2	92
5	Maltose	**5**	3	89
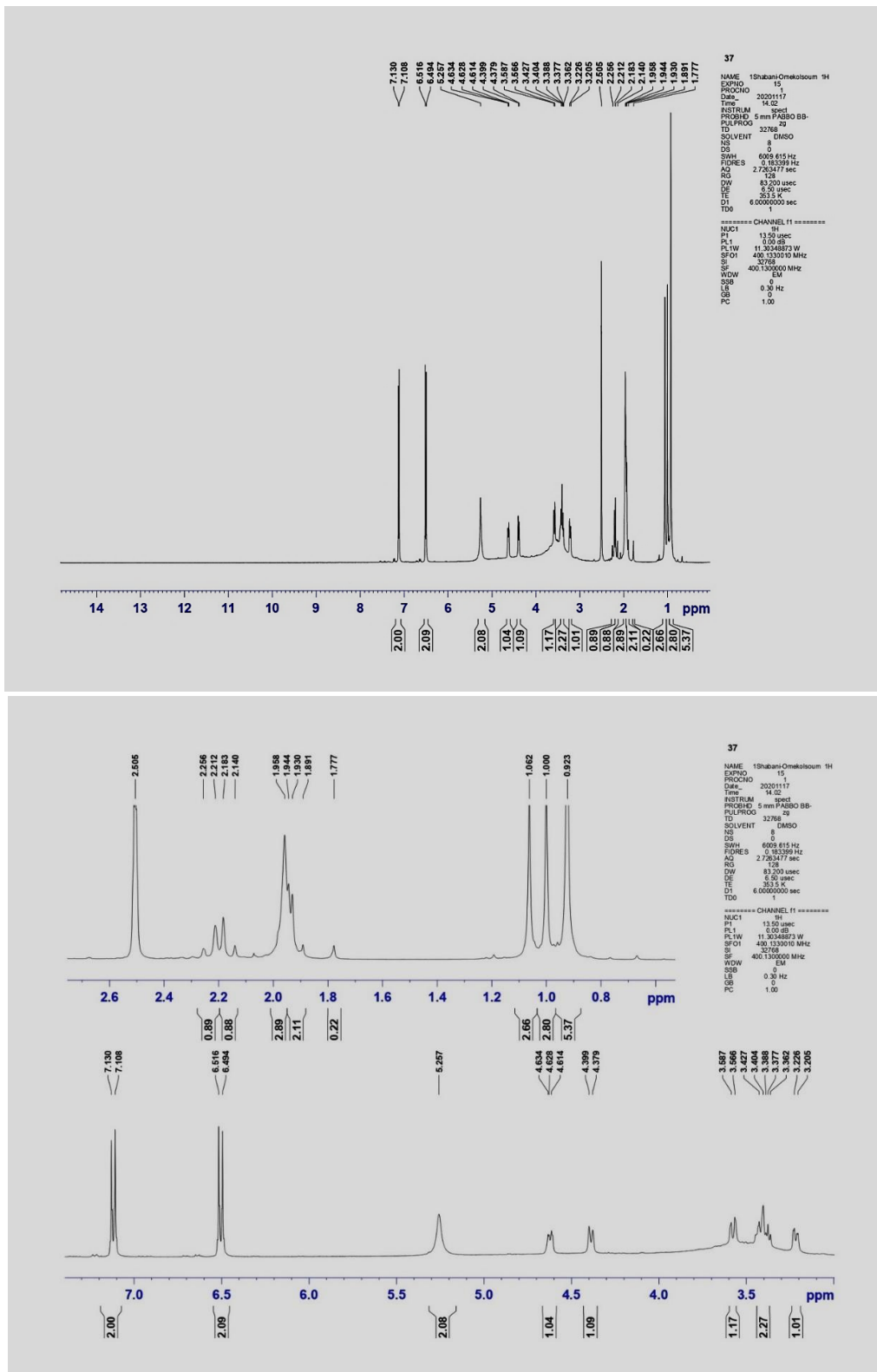
Fig. 8. ¹H NMR spectra of compound 3.
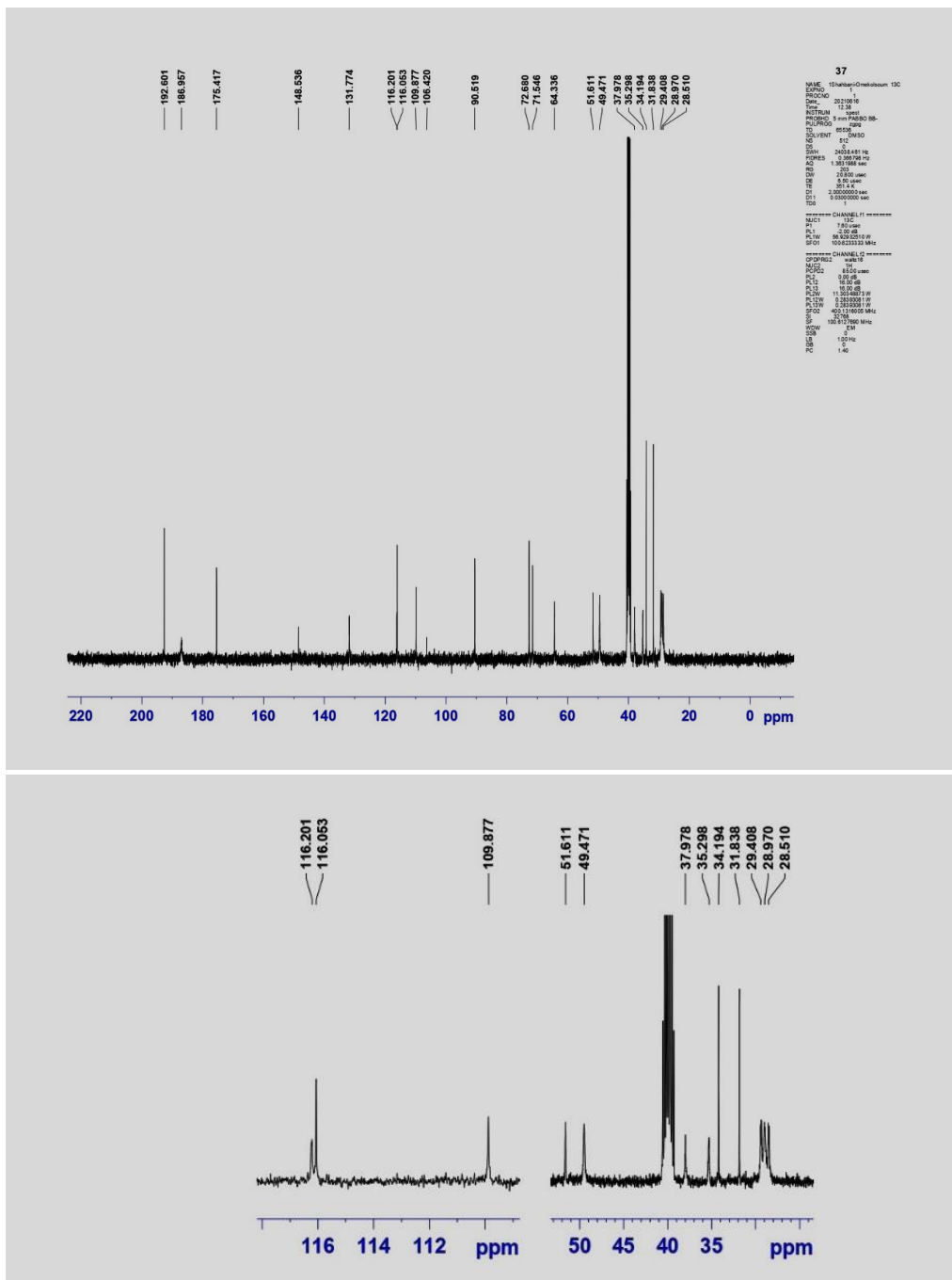
Fig. 9. ^{13}C NMR spectra of compound 3.

attributed to CO carbon groups and their enol forms have appeared at 192.60, 186,96, 176.41, and 148.53 ppm. The C, CH and CH$_{aro}$ carbon bonds have appeared at 131.77, 116.20, 116.05, 109.87, 106.42, 90.51, 72.68, 71.54, 64.33, 51.61, and 49.47 ppm.

Thereafter, we carried out the synthesis of hexahydroacridine-1,8-dione derivatives with 7 mol% of (MWCNTs)-COOH/Fe$_3$O$_4$-CaO in ethanol (Table 2).

A plausible mechanism for the reaction of 4-bromoaniline, dimedone, and sugar is envisaged

Fig. 10. A plausible mechanism for the synthesis of compound 3 using (MWCNTs)-COOH/Fe$_3$O$_4$-CaO.

Table 3. Comparison of the efficiency of different catalysts in the synthesis of compound 3 in ethanol.

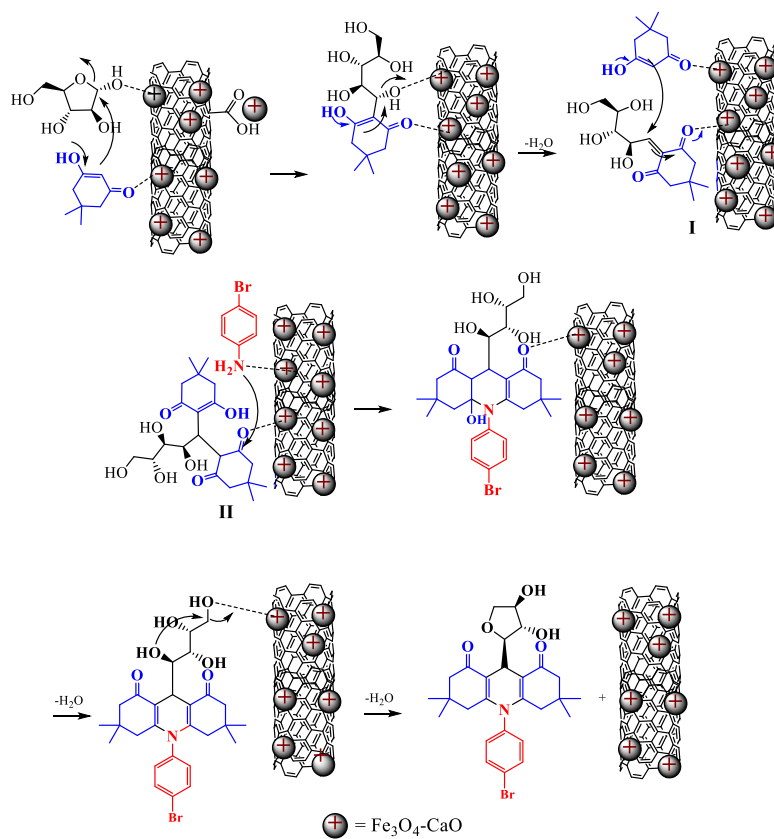| Entery	Catalyst	Amount of catalyst (mol%)	Time (hours)	Yeild %
1	Fe₃O₄ MNPs	7	4	66
2	Fe₃O₄@SiO₂-SO₃H MNPs	7	4	73
3	CaO NPs	7	4	58
4	ZnO-CaO NPs	7	4	81
5	(MWCNTs)-COOH/Fe₃O₄-CaO	7	2	95

in (Fig. 10). It is proposed that CO group of sugar is first activated by (MWCNTs)-COOH/Fe$_3$O$_4$-CaO. Nucleophilic addition of dimedone to the activated oxygen followed by the loss of H$_2$O generates intermediate I, which is further activated by (MWCNTs)-COOH/Fe$_3$O$_4$-CaO. Then, the 1,4-nucleophilic addition of a second molecule of dimedone on the activated intermediate I, in the Michael addition fashion, affords the intermediate II, which undergoes nitrogen attack of 4-bromoaniline to give 10-(4-bromophenyl)-9-((2S,3S,4R)-3,4-dihydroxytetrahydrofuran-2-yl)-3,3,6,6-tetramethyl-3,4,6,7,9,10-hexahydroacridine-1,8(2H,5H)-dione 3.

Table 4. Comparison of the efficiency of different methods in the synthesis of hexahydroacridine-1,8-dione.

Entry	Catalyst	conditions	Time (hours)	Yeild %	Ref.
1	CAN	PEG/50c	4	93-98	[46]
2	$Zn(OAc)_2$	H_2O/(reflux)	2-3	84-94	[47]
3	$CeCl_3.7H_2O$	[bmim][BF_3]/100°C	6	82-95	[48]
4	Amberlist-15	CH_3CN/reflux	4.5-6.5	90	[49]
5	[Hmim]TFA	Solvent-free/80°C	4.5-7	78-89	[50]
6	(MWCNTs)-COOH/Fe_3O_4-CaO	Ethanol	2-3	89-96	This work

Table 5. Recycling of the (MWCNTs)-COOH/Fe_3O_4-CaO.

Number of cycles	Yield[a] (%)
1	95
2	93
3	92
4	89
5	89

[a] Isolate Yield.

To investigate the efficiency of the (MWCNTs)-COOH/Fe_3O_4-CaO, we compared some other metal oxide NPs for the synthesis of compound 3 and the results were summarized in Table 3. The metal oxide NPs were synthesized according to the previously reported procedures [41-45]. As shown in Table 3, the best catalyst for the synthesis of compound 3 is (MWCNTs)-COOH/Fe_3O_4-CaO, using this metal oxide as a catalyst offers several advantages such as excellent yields, short reaction times, a simple procedure, and using ethanol as a green solvent in contrast with other metal oxides.

In order to show the advantages of this method over previously reported ones. Some of our results are compared in Table 4 to those of some other methods. These results showed that the yield, time and ratio of the present method are better or comparable to the other reported results for the synthesis of hexahydroacridin derivatives.

The catalyst was simply separated by an external magnet, washed with ethanol and water, and dried at 100 °C for 2 h. The recovered catalyst was then re-entered to a fresh reaction mixture under the same conditions and recycled 5 times without considerable loss of activity (Table 5). More recycling of the nano catalyst led to a gradual reduction during the recovering and washing steps.

CONCLUSION

In conclusion, hybrids of (MWCNTs)-COOH and Fe_3O_4-CaO NPs have been successfully fabricated in acetic acid to produce (MWCNTs)-COOH/Fe_3O_4-CaO. The structure, morphological magnetic, and surface were evaluated in details. The presence of nanoparticles and CNTs were confirmed via EDX, XRD, FT-IR. TEM and SEM. (MWCNTs)-COOH/Fe_3O_4-CaO was used as a reusable efficient catalyst for synthesis of hexahydroacridine-1,8-dione derivatives in ethanol. We have described a rapid and very efficient one-pot three component reaction between dimedone, unprotected sugars and aniline or 4-bromoaniline for the synthesis of hexahydroacridine-1,8-dione derivatives. We have demonstrated that eco-friendly, low-cost and high-yielding synthetic route towards

hexahydroacridine-1,8-dione derivatives using (MWCNTs)-COOH/Fe$_3$O$_4$-CaO. This strategy will not only give practical synthetic methods but also assures the expansion of the versatility of clean organic reactions ethanol. In addition to the intrinsic properties of nano catalysts, (MWCNTs)-COOH/Fe$_3$O$_4$-CaO hybrid showed high catalytic activity in organic reactions and increased the rate of the reaction without pollution. In addition, this study provides a new alternative to the poultry waste from the eggshell for its use in the biosynthesis of organic and heterocyclic compounds.

ACKNOWLEDGMENT

CONFLICT OF INTEREST

The authors declare that there is no conflict of interests regarding the publication of this manuscript.

REFERENCES

1. Abdoli M, Nami N, Hossaini Z. One-pot synthesis of spiro-acridine/indoline and indoline derivatives using (MWCNTs)-COOH-La$_2$O$_3$ hybrid as an effective catalyst. J Heterocycl Chem. 2020;58(2):523-533.

2. Lu Y, Yu G, Wei X, Zhan C, Jeon J-W, Wang X, et al. Fabric/multi-walled carbon nanotube sensor for portable on-site copper detection in water. Advanced Composites and Hybrid Materials. 2019;2(4):711-719.

3. Kaveh S, Nami N, Norouzi B, Mirabi A. Biosynthesis of (MWCNTs)-COOH/CdO hybrid as an effective catalyst in the synthesis of pyrimidine-thione derivatives by water lily flower extract. Inorganic and Nano-Metal Chemistry. 2020:1-12.

4. Pezeshkvar T, Norouzi B, Moradian M, Mirabi A. Fabrication of new nanocomposites based on NiO-MWCNT-sodium dodecyl sulfate in the presence of Gundelia tourneforti extract: application for methanol electrooxidation in alkaline solution. J Solid State Electrochem. 2022;26(6-7):1479-1492.

5. Heidarzadeh T, Nami N, Zareyee D. Application of (MWCNTs)-COOH/CeO$_2$ hybrid as an efficient catalyst for the synthesis of some nitrogen-containing organic compounds. Inorganic and Nano-Metal Chemistry. 2021;52(8):1173-1182.

6. Wang J, Li J, Xu X, Bi Z, Xu G, Shen H. Promising photovoltaic application of multi-walled carbon nanotubes in perovskites solar cells for retarding recombination. RSC Advances. 2016;6(48):42413-42420.

7. Goksu H, Sert H, Kilbas B, Sen F. Recent Advances in the Reduction of Nitro Compounds by Heterogenous Catalysts. Curr Org Chem. 2017;21(9):794-820.

8. Yildiz Y, Okyay TO, Sen B, Gezer B, Kuzu S, Savk A, et al. Highly Monodisperse Pt/Rh Nanoparticles Confined in the Graphene Oxide for Highly Efficient and Reusable Sorbents for Methylene Blue Removal from Aqueous Solutions. ChemistrySelect. 2017;2(2):697-701.

9. Sen B, Kuyuldar E, Demirkan B, Onal Okyay T, Şavk A, Sen F. Highly efficient polymer supported monodisperse ruthenium-nickel nanocomposites for dehydrocoupling of dimethylamine borane. Journal of Colloid and Interface Science. 2018;526:480-486.

10. Kakavandi B, Kalantary RR, Farzadkia M, Mahvi AH, Esrafili A, Azari A, et al. Enhanced chromium (VI) removal using activated carbon modified by zero valent iron and silver bimetallic nanoparticles. Journal of Environmental Health Science and Engineering. 2014;12(1).

11. Baviskar P, Chavan P, Kalyankar N, Sankapal B. Decoration of CdS nanoparticles on MWCNT's by simple solution chemistry. Appl Surf Sci. 2012;258(19):7536-7539.

12. Unal B, Senel M, Baykal A, Sözeri H. Multiwall-carbon nanotube/cobalt ferrite hybrid: Synthesis, magnetic and conductivity characterization. Current Applied Physics. 2013;13(7):1404-1412.

13. Kami D, Takeda S, Itakura Y, Gojo S, Watanabe M, Toyoda M. Application of Magnetic Nanoparticles to Gene Delivery. Int J Mol Sci. 2011;12(6):3705-3722.

14. Jenkins SI, Yiu HHP, Rosseinsky MJ, Chari DM. Magnetic nanoparticles for oligodendrocyte precursor cell transplantation therapies: progress and challenges. Molecular and Cellular Therapies. 2014;2(1):23.

15. Wong J, Prout J, Seifalian A. Magnetic Nanoparticles: New Perspectives in Drug Delivery. Curr Pharm Des. 2017;23(20).

16. Nami N, Zareyee D, Ghasemi M, Asgharzadeh A, Forouzani M, Mirzad S, et al. An efficient method for synthesis of some heterocyclic compounds containing 3-iminoisatin and 1,2,4-triazole using Fe$_3$O$_4$ magnetic nanoparticles. Journal of Sulfur Chemistry. 2017;38(3):279-290.

17. Mousavi SF, Hossaini Z, Rostami-Charati F, Nami N. Synthesis of Benzochromene Derivatives Using Reusable Fe$_3$O$_4$/ZnO Magnetic Nanoparticles: Study of Antioxidant and Antibacterial Activity. Polycyclic Aromatic Compounds. 2021;42(9):6732-6749.

18. Alinezhad H, Tollabian Z. One-Pot Reductive Amination of Carbonyl Compounds Using Sodium Borohydride-Cellulose Sulfuric Acid. Bull Korean Chem Soc. 2010;31(7):1927-1930.

19. Roopan SM, Khan FRN, Mandal BK. Fe nano particles mediated C–N bond-forming reaction: Regioselective synthesis of 3-[(2-chloroquinolin-3-yl)methyl]pyrimidin-4(3H)ones. Tetrahedron Lett. 2010;51(17):2309-2311.

20. White MA, Johnson JA, Koberstein JT, Turro NJ. Toward the Syntheses of Universal Ligands for Metal Oxide Surfaces: Controlling Surface Functionality through Click Chemistry. Journal of the American Chemical Society. 2006;128(35):11356-11357.

21. Zhu Y, Stubbs LP, Ho F, Liu R, Ship CP, Maguire JA, et al. Magnetic Nanocomposites: A New Perspective in Catalysis. ChemCatChem. 2010;2(4):365-374.

22. Al-Sabagh AM, Yehia FZ, Harding DRK, Eshaq G, ElMetwally AE. Fe$_3$O$_4$-boosted MWCNT as an efficient sustainable catalyst for PET glycolysis. Green Chem. 2016;18(14):3997-4003.

23. Göksu H, Çelik B, Yıldız Y, Şen F, Kılbaş B. Superior Monodisperse CNT-Supported CoPd (CoPd@CNT) Nanoparticles for Selective Reduction of Nitro Compounds to Primary Amines with NaBH$_4$ in Aqueous Medium. ChemistrySelect. 2016;1(10):2366-2372.

24. Helmiyati H, Masriah I. Preparation of cellulose/CaO-Fe₂O₃ nanocomposites as catalyst for fatty acid methyl ester production. PROCEEDINGS OF THE 4TH INTERNATIONAL SYMPOSIUM ON CURRENT PROGRESS IN MATHEMATICS AND SCIENCES (ISCPMS2018): AIP Publishing; 2019.

25. Ali MA, Al-Hydary IA, Al-Hattab TA. Nano-Magnetic Catalyst CaO- Fe₃O₄ for Biodiesel Production from Date Palm Seed Oil. Bulletin of Chemical Reaction Engineering & Catalysis. 2017;12(3):460.

26. Minaria M, Mohadi R. Preparation and characterization of calcium oxide from crab shells (Portunus pelagicus) and its application in biodiesel synthesis of waste cooking oil, palm and coconut oil. Science and Technology Indonesia. 2016;1(1):1-7.

27. Abd Rashid R, Shamsudin R, Abdul Hamid MA, Jalar A. Low temperature production of wollastonite from limestone and silica sand through solid-state reaction. Journal of Asian Ceramic Societies. 2014;2(1):77-81.

28. Seo JH, Park SM, Yang BJ, Jang JG. Calcined Oyster Shell Powder as an Expansive Additive in Cement Mortar. Materials. 2019;12(8):1322.

29. Lesbani A, Susi Y, Verawaty M, Mohadi R. Calcium Oxide Decomposed From Chicken's and Goat's Bones as Catalyst For Converting Discarded Cooking Oil to be Biodiesel. Aceh International Journal of Science and Technology. 2015;4(1).

30. Mohadi R, Anggraini K, Riyanti F, Lesbani A. Preparation Calcium Oxide From Chicken Eggshells. Sriwijaya Journal of Environment. 2016;1(2):32-35.

31. Singh NB, Singh NP. Formation of CaO from thermal decomposition of calcium carbonate in the presence of carboxylic acids. J Therm Anal Calorim. 2007;89(1):159-162.

32. Teixeira C, Vale N, Pérez B, Gomes A, Gomes JRB, Gomes P. "Recycling" Classical Drugs for Malaria. Chem Rev. 2014;114(22):11164-11220.

33. Gensicka-Kowalewska M, Cholewiński G, Dzierzbicka K. Recent developments in the synthesis and biological activity of acridine/acridone analogues. RSC Advances. 2017;7(26):15776-15804.

34. Martín N, Quintero M, Seoane C, Soto JL, Mora A, Suárez M, et al. Synthesis and conformational study of acridine derivatives related to 1,4-dihydropyridines. J Heterocycl Chem. 1995;32(1):235-238.

35. Hamadanian M, Jabbari V, Shamshiri M, Asad M, Mutlay I. Preparation of novel hetero-nanostructures and high efficient visible light-active photocatalyst using incorporation of CNT as an electron-transfer channel into the support TiO₂ and PbS. Journal of the Taiwan Institute of Chemical Engineers. 2013;44(5):748-757.

36. Hwa K-Y, Subramani B. Synthesis of zinc oxide nanoparticles on graphene–carbon nanotube hybrid for glucose biosensor applications. Biosensors and Bioelectronics. 2014;62:127-133.

37. Balamurugan S, Balu AR, Usharani K, Suganya M, Anitha S, Prabha D, et al. Synthesis of CdO nanopowders by a simple soft chemical method and evaluation of their antimicrobial activities. Pacific Science Review A: Natural Science and Engineering. 2016;18(3):228-232.

38. Bragg WH. The Structure of Magnetite and the Spinels. Nature. 1915;95(2386):561-561.

39. Chessin H, Hamilton WC, Post B. Position and thermal parameters of oxygen atoms in calcite. Acta Crystallogr. 1965;18(4):689-693.

40. Warren- Aver bach Applications. Industrial Applications of X-Ray Diffraction: CRC Press; 1999. p. 865-886.

41. Phiwdang K, Suphankij S, Mekprasart W, Pecharapa W. Synthesis of CuO Nanoparticles by Precipitation Method Using Different Precursors. Energy Procedia. 2013;34:740-745.

42. Ezzatzadeh E, Hossaini Z, Rostamian R, Vaseghi S, Mousavi SF. Fe₃O₄ Magnetic Nanoparticles (MNPs) as Reusable Catalyst for the Synthesis of Chromene Derivatives Using Multicomponent Reaction of 4-Hydroxycumarin Basis on Cheletropic Reaction. J Heterocycl Chem. 2017;54(5):2906-2911.

43. Nemati F, Sabaqian S. Nano- Fe₃O₄ encapsulated-silica particles bearing sulfonic acid groups as an efficient, eco-friendly and magnetically recoverable catalyst for synthesis of various xanthene derivatives under solvent-free conditions. Journal of Saudi Chemical Society. 2017;21:S383-S393.

44. Heidarzadeh T, Nami N, Zareyee D. Synthesis of Indole Derivatives Using Biosynthesized ZnO-CaO Nanoparticles as an Efficient Catalyst. Journal of Nano Research. 2021;66:61-71.

45. Varadwaj GBB, Rana S, Parida K. Cs salt of Co substituted lacunary phosphotungstate supported K10 montmorillonite showing binary catalytic activity. Chem Eng J. 2013;215-216:849-858.

46. Kidwai M, Bhatnagar D. Ceric ammonium nitrate (CAN) catalyzed synthesis of N-substituted decahydroacridine-1,8-diones in PEG. Tetrahedron Lett. 2010;51(20):2700-2703.

47. Balalaie S, Chadegani F, Darviche F, Bijanzadeh HR. One-pot Synthesis of 1,8-Dioxo-decahydroacridine Derivatives in Aqueous Media. Chin J Chem 2009;27(10):1953-1956.

48. Murugan P, Shanmugasundaram P, Ramakrishnan VT, Venkatachalapathy B, Srividya N, Ramamurthy P, et al. Synthesis and laser properties of 9-alkyl-3,3,6,6-tetramethyl-1,2,3,4,5,6,7,8,9,10-decahydroacridine-1,8-dione derivatives. Journal of the Chemical Society, Perkin Transactions 2. 1998(4):999-1004.

49. Das B, Thirupathi P, Mahender I, Reddy VS, Rao YK. Amberlyst-15: An efficient reusable heterogeneous catalyst for the synthesis of 1,8-dioxo-octahydroxanthenes and 1,8-dioxo-decahydroacridines. J Mol Catal A: Chem. 2006;247(1-2):233-239.

50. Dabiri M, Baghbanzadeh M, Arzroomchilar E. 1-Methylimidazolium triflouroacetate ([Hmim]TFA): An efficient reusable acidic ionic liquid for the synthesis of 1,8-dioxo-octahydroxanthenes and 1,8-dioxo-decahydroacridines. Catal Commun. 2008;9(5):939-942.